

Numerical Flow Analysis (NFA) Predictions of the Stability of the Joint High Speed Sealift (JHSS) Monohull in Head Seas

Kyle A. Brucker, Thomas T. O’Shea, Donald C. Wyatt, Douglas G. Dommermuth

Naval Hydrodynamics Division, Science Applications International Corporation

William R. Story

Fulcrum Corporation

Ann Marie Powers & Thomas C. Fu

Naval Surface Warfare Center, Carderock Division

ABSTRACT

The results of a set numerical simulations of the Joint High Speed Sealift (JHSS) monohull in calm water, at steady forward speed, and in head seas are presented and discussed. The majority of the paper is focussed on how steady forward speed and head seas affect the righting arm. The effect of steady forward speed on the righting arm is found to be small (+1.6%) at a 30° heel angle. The results of the head-seas simulations are compared to the results of a Froud-Krylov-type analysis based on the simulated wave field sans body. The Froud-Krylov analysis over-predicts the loss of righting moment between for wave phases 30° and 180° and has a phase-lead for wave phases between 0°-30° and 180°-360°. Visualizations from a four-degrees-of-freedom simulation of the JHSS monohull in an unstable configuration illustrate the capsizing in head seas.

KEYWORDS

Numerical Flow Analysis (NFA); Joint High Speed Sealift (JHSS); Extreme sea-states; Phase-Stability; Capsizing

INTRODUCTION

The design of current and future ships is becoming more complex with the incorporation of advanced hull forms such as the tumblehome bows and trimaran hulls currently employed in the DDG 1000 and Littoral Combat Ship (LCS) designs. In addition, these novel and advanced hull forms are operating in more extreme environments and conditions. The design and analysis process requires extrapolation from current design databases and will increasingly rely on computational tools.

The objective of this paper is to show that the Numerical Flow Analysis (NFA) software is capable of providing design support for assessing

the performance of the next generation of naval vessels undergoing extreme loads and motions while operating at high speed. To this end, the results of a systematic study of the static and dynamic roll-stability of the Joint High Speed Sealift (JHSS) monohull in head seas are presented.

The layout of the paper is as follows. The numerical approach section provides details of the hull model, computational domain, and parameters used in the study. The static stability section briefly discusses the hydrostatic stability as a baseline for comparison in following sections. The next two sections discuss the effects of steady forward speed and head seas on the righting arm curves. Specifically, a comparison to hydrostatics

based on a Froude-Krylov analysis for a fixed heel angle of 30° and the change in the righting arm as a function of wave phase (position of crest along hull) are discussed. Last, the capsizing section shows visualizations from a four-degrees-of-freedom (4DOF) simulation to illustrate the capsizing of the JHSS monohull in head seas.

NUMERICAL APPROACH

The NFA computer code is employed in this study. NFA solves the Navier-Stokes equations utilizing a cut-cell, Cartesian-grid formulation with interface-capturing to model the unsteady flow of air and water around moving bodies. The interface-capturing of the free surface uses a second-order accurate, volume-of-fluid technique. The cut-cell method is used to enforce free-slip boundary conditions on the body. A boundary-layer model has been developed (Rottman, et al., 2010), but it is not used in these numerical simulations. NFA uses an implicit Subgrid-scale model that is built into the treatment of the convective terms in the momentum equations (Rottman, et al., 2010). A panellized surface representation of the ship hull (body) is all that is required as input in terms of body geometry. The numerical scheme is implemented on parallel computers using Fortran 90 and Message Passing Interface (MPI). The interested reader is referred to Dommermuth, et al. (2007), O’Shea, et al. (2008), and Brucker, et al. (2010) for a detailed description of the numerical algorithm and of its implementation on distributed memory High Performance Computing (HPC) platforms.

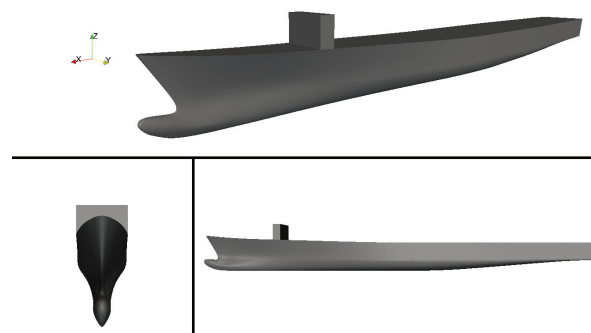


Fig. 1: NSWCCD JHSS Seakeeping Loads Model 5663 of JHSS monohull used in simulations

The Naval Surface Warfare Center Carderock Division (NSWCCD) JHSS Seakeeping Loads

Model 5663 is used for the three-dimensional numerical simulations. The model, shown in Figure 1, is 1:47.5255 scale of the full ship

Table 1 contains both full- and model-scale dimensions. The numerical simulations are normalized by the ship length ($L=6.096\text{ m}$, 240.0 inches) and the ship speed ($U=2.46\text{ m/s}$, 4.78 kts). This corresponds to a Froude Number, of $Fr = U(gL)^{-1/2} = 0.31$, which corresponds to a full-scale speed of 15.43 m/s (30 kts). It is noted that in the simulations in which the model is free to move no roll stabilization mechanisms, such as bilge keels, are present.

In all the simulations, the bow of the ship is fixed at $x=0$ and the flow is from positive x . Inflow and outflow boundary conditions are used in the stream-wise direction, and free-slip conditions are used in the cross-stream and vertical directions. The inflow condition is either a free-stream current or waves based on second-order Stokes wave theory.

Table 1: JHSS full and model scale dimensions

		Full-Scale	Model
Length	LOA	299.45 (m)	6.605 (m)
	LBP	289.72 (m)	6.096 (m)
Beam	B_{\max}	31.987 (m)	0.6730 (m)
Depth	D_{fwd}	25.543 (m)	0.5373 (m)
	D_{mid}	23.418 (m)	0.4926 (m)
Draft	T_{DWL}	8.560 (m)	0.1801 (m)
	$T_{\text{Navigational}}$	8.560 (m)	0.1801 (m)
Displacement		34,638.5 (mtons)	0.3227 (mtons)

The extents of the computational domain in the stream-wise (x), span-wise (y), and cross-stream (z) directions are respectively $[1.5L, -4L]$, $[-2L, 2L]$, and $[-1.25L, 0.75L]$. Three computational domains and time steps are employed and are herein referred to as coarse (c) medium (m) and fine (f). The number of grid points $[nx, ny, nz]$ are $[512, 256, 128]^c$, $[1024, 512, 256]^m$, and $[2048, 1024, 512]^f$. The time steps for the coarse, medium, and fine simulations are respectively $\Delta t=0.002, 0.001$, and 0.0005 . The grid points are distributed in $128 \times 64 \times 64$ blocks over 32 and 256 cores for the coarse and medium

simulations, respectively. In the fine simulation, the grid points are distributed in 128x128x64 blocks over 1024 cores. The grid is stretched with nearly uniform spacing around the ship where the grid spacing is 0.008L^c, 0.004L^m, 0.002L^f. The maximum grid spacing far away from the ship along the Cartesian axes is [0.028L, 0.073L, 0.112L]^c, [0.014L, 0.037L, 0.056L]^m, [0.006L, 0.018L, 0.028L]^f.

All simulations have been run on the Cray® (Cray Inc.) XT4 at the U.S. Army Engineering Research and Development Center (ERDC). The coarse simulations require one wall-clock hour per boat length. The medium simulations require 2.2 hours per boat length. The fine simulations require nine hours per boat length. The forces and moments are output every two iterations for all cases. This data output rate corresponds to a dimensional sampling frequency of 200Hz, 400Hz, and 800Hz for the coarse, medium and fine grids, respectively.

STATIC STABILITY

The results of a hydrostatic stability analysis of the JHSS model are presented to provide a baseline to which the stability at forward speed and in waves can be compared. Figure 2 shows the cross-section of the JHSS model at mid-ship, the water static water line (horizontal blue line), and the positions of the center of gravity, **G**, center of buoyancy, **B**, keel depth, **K**, and metacentric height, **M**. drawn to scale. The metacentric height, **M**, is calculated as

$$\overline{GM} = \overline{KB} + \overline{BM} - \overline{KG} \quad (1)$$

Based on linear theory \overline{BM} may be estimated as $\overline{BM} = I_{xx} / \nabla$, where ∇ is the volume of water displaced by the boat and I_{xx} is the moment of inertia of the water plane area. The center of buoyancy, **B**, and the moment of inertia of the water plane, I_{xx} , are computed by slicing the panellized geometry into thin strips in z and computing the appropriate contour integrals for the moments of inertia and area. These quantities are computed to check the static righting curve, as the total righting moment about the x-axis and displacement are directly output from NFA.

Hence the righting arm, \overline{GZ} , can be directly calculated as:

$$\overline{GZ} = \frac{R_M}{\Delta}, \quad (2)$$

where, R_M is the total moment about the x-axis.

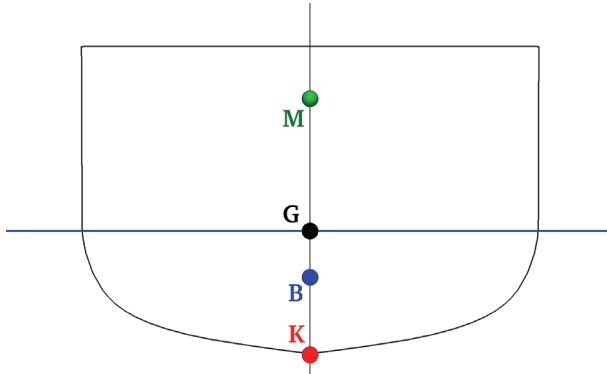


Fig. 2: The cross-section of the JHSS model at mid-ship with the hydrostatic waterline (horizontal blue line). Also shown are the positions of the center of gravity, **G**, center of buoyancy, **B**, keel depth, **K**, and meta-centric height, **M**.

The hydrostatic righting arm curve in Figure 3 is created by rolling the model in small angular increments and then iteratively sinking and trimming the rotated model until it is in hydrostatic equilibrium. This hydrostatically balanced, rotated, sunk and trimmed model is used as the input for the steady forward speed and head seas studies. Figure 3 shows the hydrostatic stability curves and the approximations $\overline{GM}\phi$ and $\overline{GM} \sin(\phi)$. The results are shown for various vertical centers of gravity (VCG), as the 4DOF simulation uses a more unstable VCG position. All other simulations use VCG=0, i.e., at the static water line.

EFFECT OF STEADY FORWARD SPEED

The effect of steady forward speed on the righting arm is considered for a heel angle of 30°. Figure 4 serves a dual purpose; the first is to illustrate that the solution converges as the grid is refined, and the second is to show the correction to the righting moment that occurs when the unsteady two-phase flow around the hull is included. The coarse (black), medium (red), and fine (blue) results are shown in addition to the hydrostatic righting arm (dashed black line). Between $T=0$ and $T=2$, the

flow is accelerated from rest to the free-stream value. After the initial transient, the righting arm increases to $0.01266L$ a 1.6% gain over the hydrostatic value.

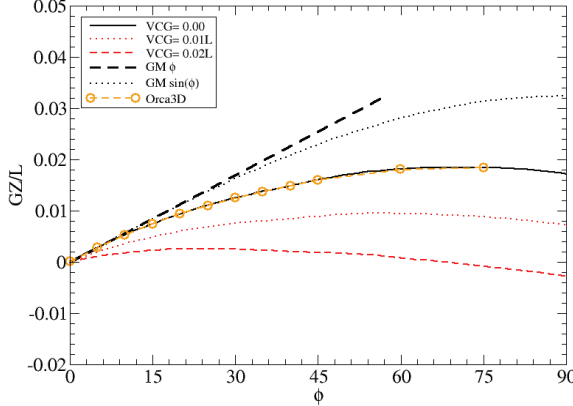


Fig. 3: Righting arm as a function of heel angle. Also shown in red are the changes with respect to the position of the vertical center of gravity (VCG).

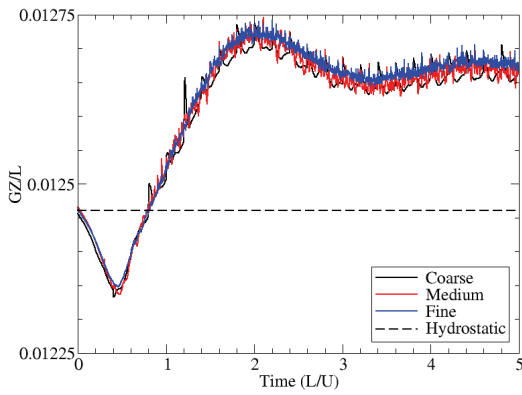


Fig. 4: The effect of steady forward speed on the righting arm at 30° heel. The grid resolutions and time steps corresponding to coarse, medium, and fine results are given in the Numerical Approach section.

STABILITY IN WAVES

All simulations that are discussed hereafter are in waves. The wavelength, λ , is equal to the ship length ($\lambda=L$), and the amplitude, a , of the waves is $a=0.015L$. The waves are specified over a region of $0.5L$ at the front of the domain based on second-order Stokes wave theory (Ratcliffe, et al., 2008). The waves then travel towards the ship where the full interaction of the ship and waves is simulated. The NFA results include the effects of wave radiation and diffraction. To quantify the effects wave radiation and diffraction, a

simulation of the waves with no body is performed and the resulting pressure field is used to calculate the Froude-Krylov force on the body.

The results of an NFA simulation of the JHSS monohull at a fixed heel angle of 30° in waves with $\lambda=L$ and $a=0.015L$ at the medium grid resolution are discussed in figures 5-7. Figure 5 compares the hydrostatic righting arm calculated based on the Froude-Krylov force to the righting arm from NFA. In the subsequent discussion, the wave phase, θ , is as follows: zero phase is defined as the phase when the crest of the wave is at the bow. Comparing the positive and negative changes to the righting arm in figure 5, the Froude-Krylov prediction is in better agreement for gains to the righting arm ($\theta = 0^\circ - 30^\circ, 180^\circ - 360^\circ$), albeit with a phase-lead. The prediction for losses to the righting arm are over-predicted. The maximum over prediction is 7% and occurs at $\theta = 130^\circ$.

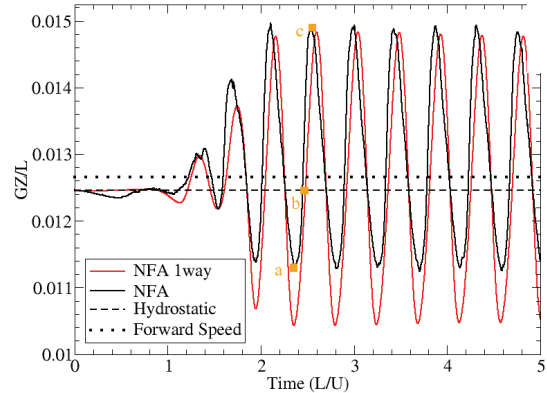


Fig. 5: Comparison of righting arms as a function of wave phase (time) for 30° heel. The two-way coupled NFA predictions are shown in black. The one-way couple NFA predictions based on a Froude-Krylov force are shown in red. The points labeled a, b and c correspond to the waves shown in figure 6

Figure 6 shows the waves when (a) the maximum loss in righting arm occurs, (b) the righting arm is equal to the hydrostatic righting arm, and (c) the maximum gain in righting arm.

Figure 7 shows the stacked data from six full wave periods (open circles) plotted along with the average over all six wave periods (solid black line). The six wave periods were all after $T=2$ when fully developed waves were along the entire length of the boat. The phase average is in good agreement with the instantaneous values.

The results of NFA simulations at heel angles of $10^\circ, 20^\circ, 30^\circ, 40^\circ, 50^\circ$, and 60° with the same waves and at the medium grid resolution are used to construct figures similar to figure 7. These plots are used to construct figure 8. Figure 8 shows the change in righting arm as a function of heel angle, for lines of constant wave phase. The maximum righting arm lost, -10% , occurs at a heel angle of 60° and phase angle of 120° . The maximum righting arm gained, $+10\%$, occurs at a heel angle of 60° and phase angle of 300° .

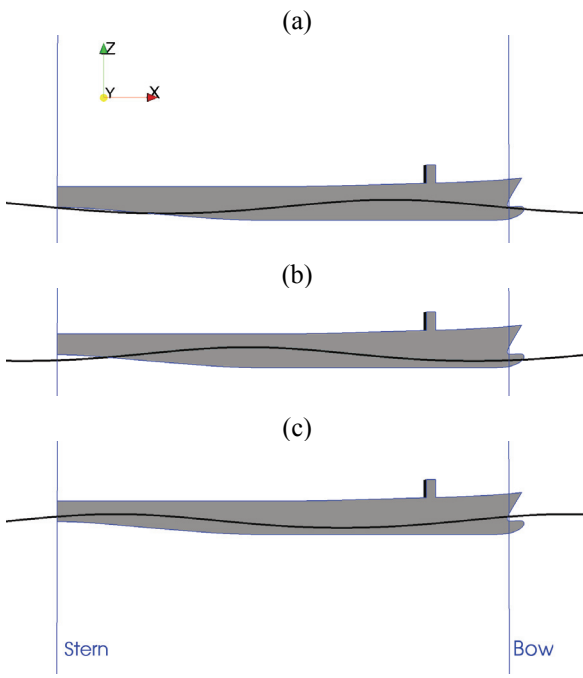


Fig. 6: Position of waves when (a) maximum loss to righting arm, (b) no loss or gain to righting arm, (c) maximum gain to righting arm.

CAPSIZING

Attention is now focussed on the results of a 4DOF simulation. The JHSS monohull model at 0° initial heel is put in waves and free to sway, heave, roll, and pitch. Without propulsion and rudders, surge and yaw would allow the model to be pushed parallel to the waves and exit out of the domain, and hence both are fixed at zero for the simulations.

Based on the hydrostatic stability plot, the vertical position of the center of gravity ($VCG=0.025L$ above the mean water line) was chosen so that roll of more than $\sim 30^\circ$ should allow

for capsizing only when additional losses to the righting arm due to wave interactions occur. Figure 9 shows a time series of renderings from the 4DOF simulation illustrating the capsizing in head seas.

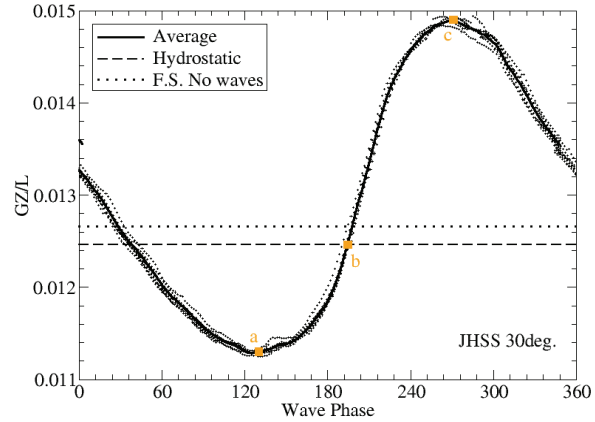


Fig. 7: The effect of waves on the righting arm at 30° heel. Data (shown as open circles) is from six wave periods. The solid black line is the average, the dashed black line is the hydrostatic righting arm, and the dotted black line is the righting arm at steady forward speed. The points labeled a, b and c correspond to the waves shown in figure 6.

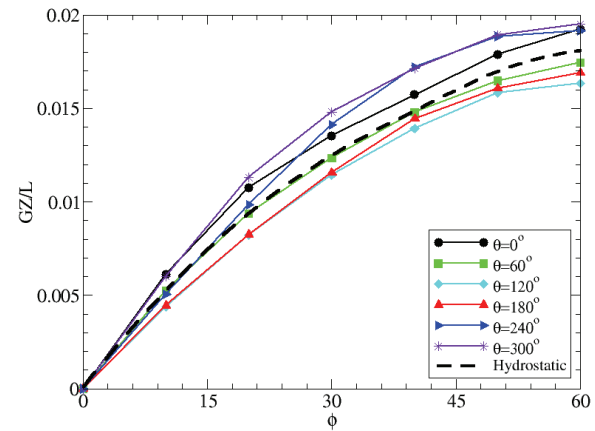


Fig. 8: Change in righting arm as a function of heel angle with lines of constant wave phase. The hydrostatic righting arm curve (---) is plotted for comparison.

CONCLUSIONS

The results of a set of NFA simulations of the JHSS monohull in calm water at steady forward speed and in head seas are presented and discussed. The change in righting arm due to steady forward speed at a fixed heel angle of 30°

was found to be 1.6%. Differences between the hydrostatic righting arm based on the Froud-Krylov predictions and the numerical simulations are observed. The hydrostatic Froud-Krylov predictions for gained righting arm are in agreement with respect to amplitude but show a phase lead when compared to the numerical simulations. For a heel angle of 30° the Froud-Krylov force predictions for lost righting arm are over-predicted. The maximum over-prediction is 7% and occurs at a wave phase of 130°. For a 60° heel angle, the over prediction is 10% and occurs at a wave phase of 120°.

ACKNOWLEDGMENTS

This work was supported by the Office of Naval Research, under the direction of Dr. Paul Hess, III. The authors would like to acknowledge Art Reed, Ph.D., for his insightful discussions and guidance during the planning and preparation of the paper. The authors would like to thank Scott Grahm for performing the Orca 3D calculations.

The Carderock Division, Naval Surface Warfare Center (NSWCCD) supports this research. This research is also supported by SAIC internal R&D funding. NFA predictions are supported in part by a grant of computer time from the Department of Defense High Performance Computing Modernization Program (HPCMP). NFA simulations have been performed on the Cray XT4 at the U.S. Army Engineering Research and Development Center.

REFERENCES

Brucker, K. A., O’Shea, T. T., Dommermuth, D. G., & Adams, P. (2010). “Three-dimensional simulations of Deep-Water breaking waves”, Proc of the 28th Symp. on Naval Hydrodynamics, Pasadena, California, USA.

Dommermuth, D. G., O’Shea, T. T., Wyatt, D. C., Ratcliffe, T., Weymouth, G. D., Hendrikson, K. L., Yue, D. K., Sussman, M., Adams, P., & Valenciano, M. (2007). “An application of cartesian-grid and volume-of-fluid methods to numerical ship hydrodynamics”, Proc. of the 9th Intl Conf on Numerical Ship Hydrodynamics, Ann Arbor, Michigan.

Drazen, D. A., Fullerton, A. M., Fu, T. C., Beale, K. L.C., O’Shea, T. T., Brucker, K. A., Wyatt, D. C., Bhushan, S., Carrica, P. M., & Stern, F. (2010). “Comparisons of model-scale experimental measurements and computational predictions for the transom wave of a large-scale transom model”, Proc. 28th Symp. on Naval Hydrodynamics, Pasadena, California, USA.

O’Shea, T. T., Brucker, K. A., Dommermuth, D. G., & Wyatt, D. C. (2008). “A numerical formulation for simulating free-surface hydrodynamics”, Proc. of the 27th Symp. on Naval Hydrodynamics, Seoul, Korea.

Ratcliffe, T., Minnick, L., O’Shea, T., Fu, T., Russell, L., and Dommermuth, D. (2008). “An integrated experimental and computational investigation into the dynamic loads and free-surface wave-field perturbations induced by head-sea regular waves on a 1/8.25 scale-model of the R/V Athena”, Proc. of the 28th Symp. on Naval Hydrodynamics, Seoul, Korea.

Rottman, J. W., Brucker, K. A., Dommermuth, D. G., & Broutman, D. (2010). “Parameterization of the internal-wave field generated by a submarine and its turbulent wake in a uniformly stratified fluid”, Proc. 28th Symp. on Naval Hydrodynamics, Pasadena, California, USA.

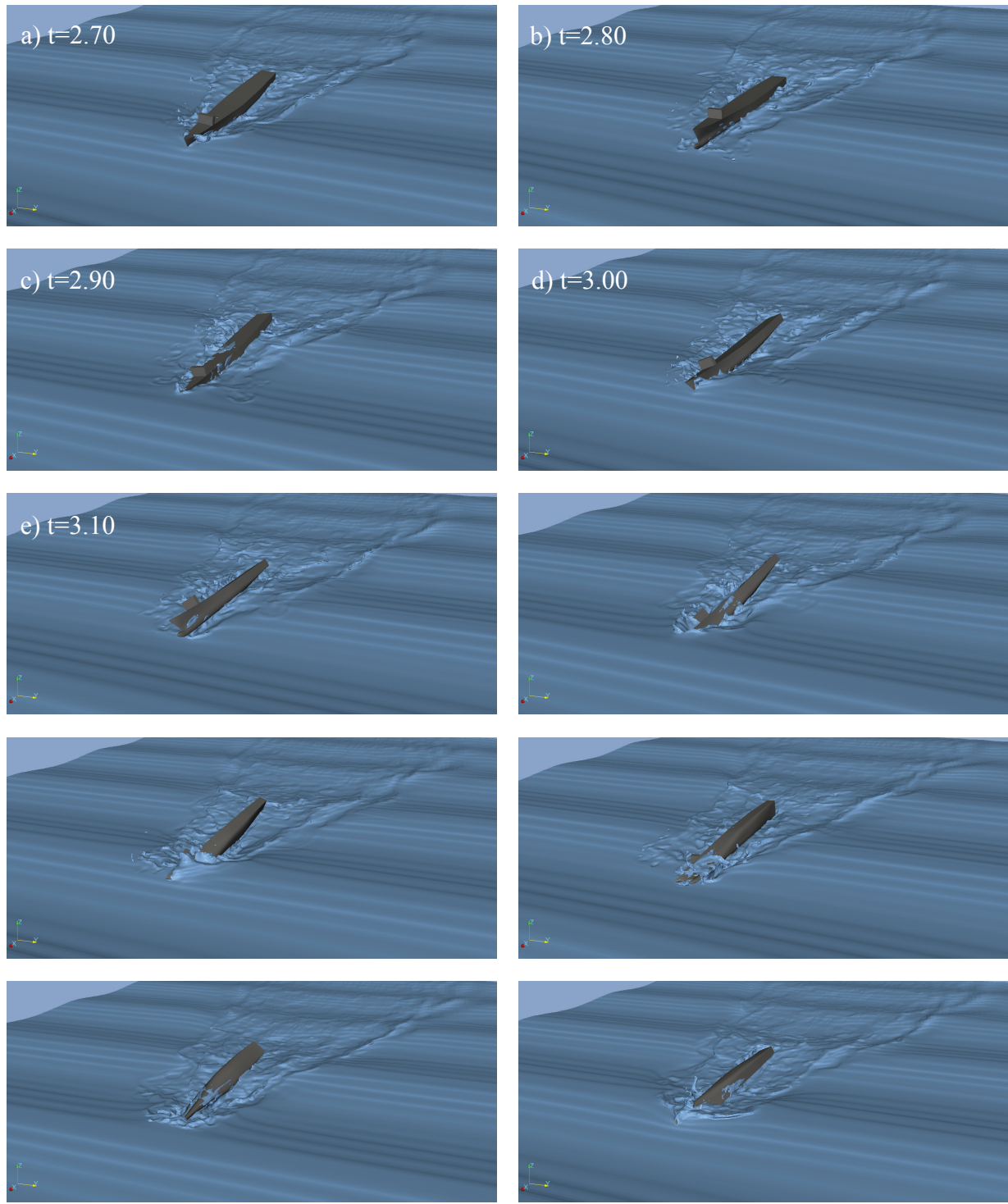


Fig. 9: Instantaneous visualizations of a 4DOF simulation of the JHSS monohull in head-seas with $\alpha=0.015L$ and $\lambda=L$, where L is the ship length, λ is the wave length, and α is the wave amplitude